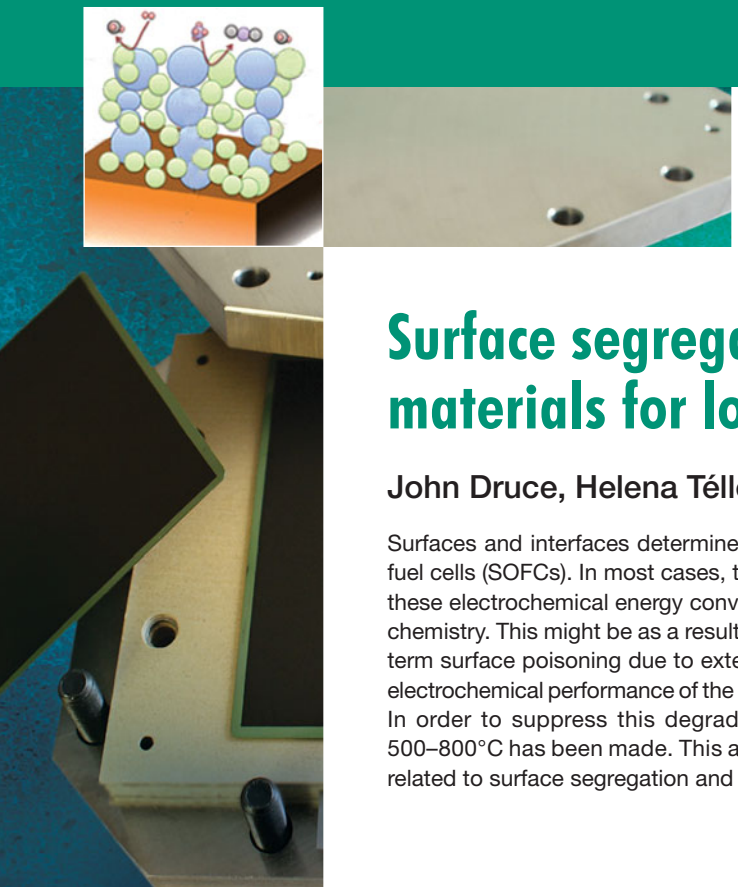


# Surface segregation and poisoning in materials for low-temperature SOFCs

John Druce, Helena Téllez, and Junji Hyodo

Surfaces and interfaces determine the performance and long-term durability of solid-oxide fuel cells (SOFCs). In most cases, the surface chemical composition of the materials used in these electrochemical energy conversion devices shows significant deviations from the bulk chemistry. This might be as a result of surface cation segregation processes, as well as long-term surface poisoning due to external impurities. Both processes have implications for the electrochemical performance of the devices, leading to the degradation of the cell components. In order to suppress this degradation, an effort to lower the operation temperature to 500–800°C has been made. This article provides an overview of present research progress related to surface segregation and poisoning for low-temperature SOFCs.

## Introduction

As commercial implementation of solid-oxide fuel cells (SOFCs) approaches, a better understanding of the surface chemistry and the processes leading to long-term performance degradation is required. The surface composition governs the kinetics of oxygen exchange between the gas phase and the mixed ionic-electronic conducting electrodes (see the Introductory article in this issue). This reaction, involving the adsorption of an oxygen molecule, its subsequent dissociation, ionization, and finally incorporation of oxygen ions into the ceramic is often the rate-limiting step for performance. Moreover, mass transport across the electrode-electrolyte interface also contributes a non-negligible resistance to the overall cell behavior, which points to the importance of the surface composition of the electrolyte for the operation of the SOFC.

However, the electrochemically active surface and interfaces in SOFCs are generally very different from the bulk chemical compositions for virtually all materials commonly used for SOFCs, and ultimately will determine the performance and long-term durability of the devices.

Several processes might contribute to the changes in the surface chemistry at low and intermediate operating temperatures (500–800°C), such as cation segregation and external surface poisoning, affecting all the components of the SOFCs (electrolytes, cathodes, and anodes). In this article, we discuss these processes and how they might affect the electrocatalytically active surfaces and interfaces, with strong implications for SOFC performance and durability.

## Electrolytes

By far, the most widely employed electrolytes in SOFC technologies are those with a fluorite structure, such as $Zr_{1-x}Y_xO_{2-x/2}$ (YSZ) and substituted cerium dioxide (i.e., $Ce_{1-x}RE_xO_{2-x/2}$), where RE is a rare-earth element. Perovskite structured electrolytes, such as those based on substituted lanthanum gallate (e.g., $(La,Sr)(Ga,Mg)O_{3-\delta}$, (LSGM)), are also of interest. However, these perovskite-based electrolytes show similar trends (e.g., segregation of $Sr^{2+}$ upon annealing[1]) to those that will be discussed for the electrode materials (also typically perovskite-based) later.

Similar to the well-studied phenomenon of impurity segregation to grain boundaries in polycrystalline ceramic samples,[2] the surfaces of fluorite-structured electrolytes after high-temperature treatment are coated with impurities, typically Ca, but also Na, Si, Al, as well as some transition metals.[3–6] Studies using low energy ion scattering spectroscopy, which selectively analyzes only the very outer layer of atoms of a surface, showed that after calcination at 1000°C for five hours (i.e., comparable to the heat treatment that may be used to

John Druce, International Institute for Carbon Neutral Energy Research, Kyushu University, Japan; john.druce@i2cner.kyushu-u.ac.jp
Helena Téllez, International Institute for Carbon Neutral Energy Research, Kyushu University, Japan; htellez@i2cner.kyushu-u.ac.jp
Junji Hyodo, Department of Applied Chemistry, Kyushu University, Japan; hyodo_j@cstf.kyushu-u.ac.jp
DOI: 10.1557/mrs.2014.170


© 2014 Materials Research Society
https://doi.org/10.1557/mrs.2014.170 Published online by Cambridge University Press

sinter an electrode onto the electrolyte), neither Y or Zr was evident in the outer atomic surface layer of YSZ ceramics (produced from commercially pure powders), which was instead completely covered by a monolayer thick film of impurities, predominantly calcium.[4] X-ray photoelectron spectroscopy (XPS) analysis of the chemical states in surface films of segregated impurities suggested that these films consist of a silicate-type phase, with some dissolved Y and Na (and other cations).[3] Samples annealed at lower temperatures of 500–700°C showed similar segregation, although the surfaces were not fully covered after one hour of annealing, which suggests some kinetic limitation.[4]

The link between segregation of impurities to grain boundaries and surface segregation in fluorites was illustrated by a study using time-of-flight secondary ion mass spectrometry (ToF-SIMS) to analyze YSZ polycrystalline ceramics.[6] The surface of a sample after annealing was covered by the impurities mentioned previously. As the surface layers were progressively removed by sputtering, the impurity coverage was seen to recede toward the grain boundaries. This suggests a mechanism as illustrated in **Figure 1**a, where the impurities first segregate to the grain boundaries, along which they are transported to the surface and emerge out of the grain boundaries to spread across the surface, creating a uniform film of monolayer thickness. While bulk oxygen diffusion is fast in the materials of interest, cation diffusion in the bulk is typically much slower, with the dominant mechanism being via a grain boundary pathway.[7,8]

Note that much of the analyses referred to previously were conducted on "bulk" polycrystalline ceramic specimens, essentially concentrating on the effects of temperature, and neglecting any possible changes during device operation under current flow. More recent studies on patterned microelectrodes on polycrystalline YSZ have shown similar behavior,[9,10] and even suggest qualitatively more silicon segregation in electrode areas surrounding a $(La_{0.75}Sr_{0.25})_{0.95}MnO_3$ (LSM) microelectrode subjected to electrochemical testing compared to those surrounding untested LSM microelectrodes with the same thermal history.[10]

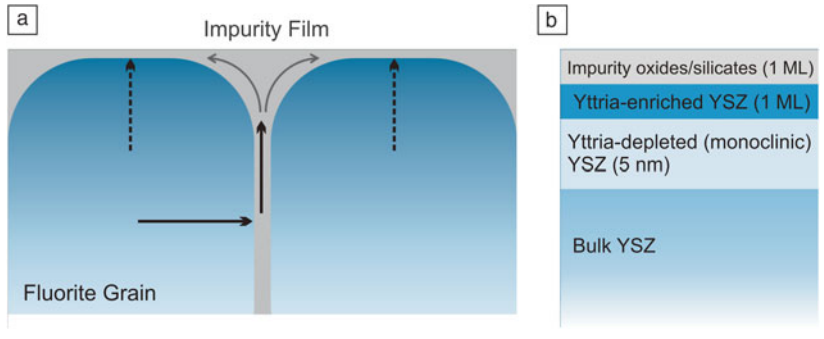



**Figure 1.** Schematics of (a) segregation mechanism of oxide impurities (gray) (adapted from Reference 6). Impurities first segregate to the grain boundaries, along which they can move rapidly toward the surface, where they emerge and wet the surface. (b) Near-surface structure (adapted from Reference 14) of YSZ fluorite electrolytes. ML, monolayer.

As might be expected, the glassy films of segregated impurity oxides block the incorporation of oxygen, as demonstrated by de Ridder et al.,[4] who used $^{18}O$ isotope exchange experiments on YSZ to reveal that the rate of the reaction was inversely proportional to the impurity coverage of the samples. This implies that the "intrinsic" surface exchange coefficient of YSZ may be higher than often measured, and is in fact limited by the blocking effect of this ubiquitous layer of segregated impurities.

One method to ameliorate this blocking effect may be to use surface additives that scavenge surface impurities, in a similar way to those used for grain boundary impurities.[11,12] For example, treatment of the surface of $Ce_{0.9}Gd_{0.1}O_{1.95}$ with $La_2O_3$ increased the surface exchange coefficient by a factor of 50, which was attributed to this type of "cleaning" mechanism.[13]

The segregation of aliovalent substituents (e.g., Y in YSZ,[3,14] or RE in $(Ce,RE)O_2$, RE = Sc, La, Gd)[5,15,16] has also been both observed experimentally and predicted computationally.[17,18] However, computational predictions neglect the presence of impurities at low (e.g., ppm) concentrations in "real" materials, and so indicate the rare-earth cation present in the very outer layer. In contrast, experimental observations show rare-earth enrichment in the layers beneath the impurity film discussed previously. The resulting structure may resemble that shown in Figure 1b, where the surface enrichment of the rare-earth element leaves a rare-earth deficient subsurface region.[14] In the case of YSZ, this rare-earth depleted region may revert to monoclinic zirconia, accompanied by a significant decrease in oxygen diffusivity.

Even in materials in which there is no structural change, such as those based on $CeO_2$, which is already cubic in its pure form, the segregation of aliovalent substituents could also affect transport properties in the near surface by causing local redistribution of oxygen vacancies.[15,18]

## Cathodes

### *Surface segregation*

The surface chemistry of cathode materials for SOFCs has been a pivotal research topic aiming to elucidate the mechanisms of oxygen reduction and subsequent incorporation into the electrode, which ultimately determines the performance of the cathode.[19]

The preferential segregation of aliovalent cations in perovskite materials was first reported by Teraoka et al. in 1988,[20] who studied Sr enrichment in $La_{1-x}Sr_xCoO_{3-\delta}$ (LSC) when treated at temperatures above 500°C. This work showed that the surface chemistry is drastically modified, depending on the processing conditions used (e.g., oxygen partial pressures, temperature), and accompanied by a decrease in the catalytic activity of the material with Sr-segregation. Since then, many other authors have shown similar findings in Sr-doped cathodes at elevated temperatures and/or under electrochemical polarization (e.g., $La_{1-x}Sr_xCo_{1-y}Fe_yO_{3-\delta}$ [LSCF],[21–25]



https://doi.org/10.1557/mrs.2014.170 Published online by Cambridge University Press

$Sm_{1-x}Sr_xCoO_{3-\delta}$,[26] $La_{1-x}Sr_xMnO_{3-\delta}$[27–29]). Furthermore, the segregation of other divalent cations has been reported in other perovskite and perovskite-based materials, such as $Pb^{2+}$ in (La,Pb)$MnO_{3-\delta}$[30] or $Ba^{2+}$ in (Ln,Ba)$Co_2O_{5+\delta}$ double perovskites.[31,32]

Many of the described studies were performed at relatively high temperatures (T > 600°C) for significant amounts of time. Nevertheless, recent investigations revealed that this segregation can take place short-term and at relatively low temperatures. For instance, Sr segregation takes place in LSCF after annealing in oxygen at 400°C for 8 h (**Figure 2**),[23] whereas Ba segregation in $GdBaCo_2O_{5+\delta}$ double perovskites starts after annealing for just 15 minutes at 400°C.[32]

The changes in the surface states that occur upon cation segregation may have a detrimental effect on the oxygen surface exchange kinetics. For instance, the increase in surface polarization resistance ($R_s$) associated with oxygen exchange at the electrode surface in LSC microelectrodes on YSZ was correlated with a higher Sr enrichment of the electrode surface after annealing at 600°C in air for 72 h.[25]

Further degradation of the cathode surface might occur due to the formation of secondary phases and/or reaction of the segregated species with the surrounding gas phase (e.g., SrO/SrOH particles or other perovskite-related phases with different stacking sequences, such as layered Ruddlesden-Popper type structures of the form $A_{n+1}B_nO_{3n+1}$). Bucher et al.[22] reported that the chemical surface exchange coefficient $k_{chem}$ in LSCF at 600°C decreased by a factor of two in dry $O_2$, although exposure to a humidified atmosphere for 1000 h leads to a further decrease by a factor of 10. This degradation was related to the formation of a 10-nm-thick Sr-rich silicate layer in the presence of humidity.

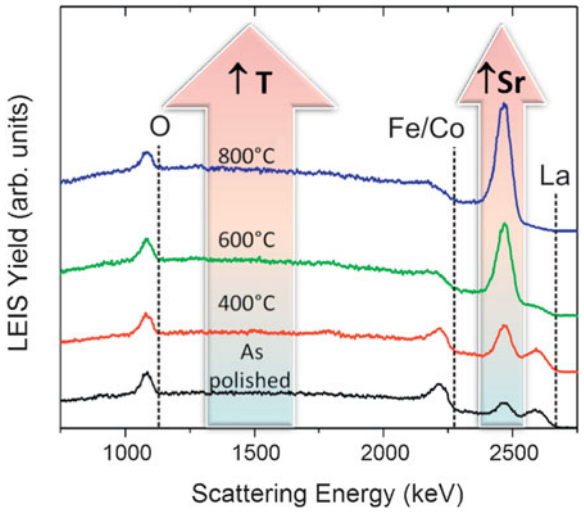



**Figure 2.** Evolution of the outermost surface of a $La_{0.6}Sr_{0.4}Co_{0.2}Fe_{0.8}O_{3-\delta}$ cathode annealed in air for eight hours as a function of the annealing temperature. The surface concentration of Sr increases with annealing temperature, indicating segregation of that element from the bulk. LEIS, low energy ion scattering. Reprinted with permission from Reference 23. © 2013 Elsevier.

Nevertheless, the effects of Sr segregation on the surface exchange properties are not yet fully understood, with some studies even suggesting that it can be a positive phenomenon. Sase et al. reported an enhancement of the oxygen surface exchange kinetics at 500°C taking place at the interface of the perovskite (La,Sr)$CoO_{3-\delta}$ ($LSC_{113}$) and the Ruddlesden-Popper $(La,Sr)_2CoO_{4\pm\delta}$ ($LSC_{214}$ ) compared to the respective single constituents.[33,34] The origin of such an improvement is unclear, although some theoretical and experimental results related it with Sr segregation from $LSC_{113}$ to $LSC_{214}$, leading to an increased oxygen vacancy concentration in the $LSC_{214}$ phase near the interface.[35,36] This improved interfacial behavior opens new possibilities to design novel heterostructures with better performance (e.g., $LSC_{214}$-decorated $LSC_{113}$[37]).

Given that this is a common process taking place under the operational conditions of the cathode materials, there are increasing efforts aimed toward understand the driving forces for cation segregation and how it can be suppressed or promoted.[38,39] First, segregation of the divalent cations neutralizes the polar surface that would otherwise occur for perovskites in which both of the host cations have a 3+ charge (e.g., $La^{3+}Co^{3+}O_{3-\delta}$).[40,41] The presence of oxygen vacancies at the surface and space-charge effects at the near-surface are also likely to contribute to this surface segregation. Second, elastic interactions due to cation size mismatch with the surrounding host lattice and chemical expansion effects will also be present.[39] The mechanism for cation segregation is, therefore, quite complex and many other factors (e.g., presence of impurities, microstructure, atmosphere, and temperature) may also have an important effect and should be addressed.[32,42]

## Cathode poisoning

One of the main causes for the degradation of cathode performance in real SOFC stacks is poisoning of the electrode surface.[43,44] For example, volatile oxyhydroxide Cr species arising from the Fe-Cr alloys used as electrical interconnects between cells, or balance-of-plant components such as heat exchangers,[45,46] react with segregated Sr to form $SrCrO_4$ oxides that passivate the cathode surface. Jiang and Chen[47] have recently reviewed much of the work on this topic over the last decade.

Small concentrations (e.g., a few ppm) of $SO_2$ in feed air may react with Sr from the cathode to form $SrSO_4$ and decrease electrode performance, especially for cobalt-containing electrode materials.[48–50] Carbon dioxide in air supplied to the cathode can also lead to a (recoverable) degradation in (Ba,Sr)(Co,Fe)$O_{3-\delta}$ (BSCF)-based electrodes, attributed to the formation of carbonates at the electrode surface.[51]

Other sources of impurities that can lead to similar poisoning effects include boron from borosilicate glasses used as seals for gas-tightness,[52] and silica originating both from glass seals and from siloxane greases in valves in the gas handling system.[21,22] The latter is exacerbated by humid atmospheres, which promote the formation of volatile $Si(OH)_4$, which is subsequently transported to the electrode surface where it poisons the electrodes.[22]


https://doi.org/10.1557/mrs.2014.170 Published online by Cambridge University Press

In many cases, the poisoning species have a high affinity to react with the segregated cations, as described previously; for example, Cr or S reacting with segregated Sr to form $SrCrO_4$ or $SrSO_4$, respectively.[53,54] Therefore, Sr-free materials, such as the (undoped) Ruddlesden-Popper $La_2NiO_{4+\delta}$ phase may show more tolerance to many of these poisons[55] and they warrant further investigation to mitigate the deleterious effects of electrode poisoning.

## Anodes

At the anode of the SOFC, a hydrogen or hydrocarbon fuel is directly oxidized to generate electricity. To facilitate this, the anode must possess high mixed ionic-electronic conductivity and high catalytic activity for oxidation. The latter suggests the importance of studying the surface chemistry to understand the reactions at the anode and the design of improved LT-SOFC anode materials and structures.

Broadly, SOFC anodes can be broken into three classes: metallic, ceramic, and ceramic-metal composite ("cermet").[56–59] **Figure 3** shows a schematic representation of a typical Ni-YSZ cermet anode, which gives good electrochemical performance and is stable in reducing atmospheres. Even though much knowledge has been gained from previous studies on the mechanisms of reactions at this anode, the Ni-YSZ cermet anode is still far from straightforward in terms of its surface properties.

### Segregation in anodes

As discussed in the electrolyte section, the outermost surface of heat treated YSZ is covered with impurities, including Ca, Si, and Na.[4,14] Segregation of these impurities also occurs at the surface of YSZ in a Ni-YSZ cermet anode.[60] Furthermore, anode materials are exposed to highly reducing atmospheres of hydrogen or hydrocarbon fuels, operating in oxygen partial pressures lower than ~$10^{-20}$ atm, which will undoubtedly affect the surface state and, in turn, may affect the catalytic performance of the anode. However, there are as yet few specific studies of the effects of such reducing atmospheres on surface segregation to clarify this behavior.

In addition, the nature of the surface of the catalytically active Ni is important for anode performance. Commercially available nickel metal typically contains a variety of impurity species, which increase its electronic resistance, and may cause decreased anode performance.[60,61] The impurities also affect the YSZ surface microstructure and segregation behavior at the contact interface between Ni metal and YSZ.[60–62] This solid-solid interface is one of the aspects that increases the complexity of cermet anode surfaces. Relaxation of surface energy is generally considered to be the driving force for surface segregation.[41] The interfacial energy at the Ni-YSZ contact is likely to be different from that of the YSZ-fuel surface, which may modify the driving force for, and hence extent of, surface segregation and, in turn, performance of the anode. In fact, there are several reports of segregation of Si and of changing morphologies at the Ni-YSZ interface.[62–64] Figure 3 shows a transmission electron microscopy image of segregated Si at the Ni-YSZ interface,[64] which has been shown to lead to an increase in the resistance of the anode.[62–64] The active site for the anode reaction is the triple phase boundary (TPB), where the three phases carrying the reactants (i.e., fuel in the gas phase, oxygen in the ionically conducting YSZ, and electrons in the electronically conducting Ni) are brought together. However, the nature of the surfaces in the region of the TPB is further complicated because, as well as the TPB itself, the surrounding region contains three different types of interfaces (i.e., fuel-YSZ, fuel-Ni, and YSZ-Ni), as shown in Figure 3.Therefore, understanding the segregation behavior and composition at the TPB and surrounding region will provide useful insights into the nature of this reaction and guide researchers in tailoring the surface properties of cermet anodes for improved electrochemical performance.

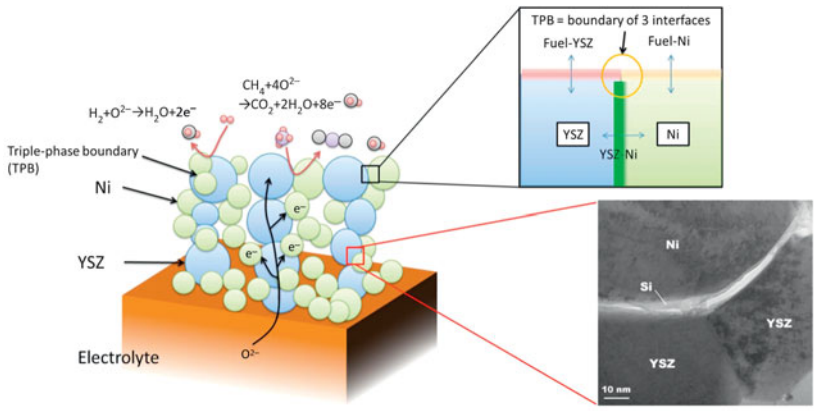



**Figure 3.** Schematic illustration of the reaction at the Ni/yttria-stabilized zirconia (YSZ) cermet anode. The top inset shows an expanded view of the triple-phase boundary (TPB) region, which contains three types of interface (i.e., Ni-YSZ, Ni-fuel, and YSZ-fuel). A transmission electron microscope (TEM) image shows the segregation of Si impurities to the interface between Ni and YSZ. TEM image reprinted with permission from Reference 71. © 2003 Elsevier.

### Anode poisoning

As for cathode materials, the anode environment also contains some sources that can lead to poisoning of the anode surface. Many experimental observations of poisoning, mainly by Si, B, Cl, and S originating from the fuel and sealing materials[48,65–69] and carbon deposition from fuels,[70–75] have been reported. Because the SOFC can run on various kinds of fuel, each of which contains different impurity species, the effects of these impurities in fuels on anode properties has been especially well studied.

Sulfur is one of the most commonly occurring poisoning species found in fuels for SOFCs, and especially those based on fossil fuels can have significant deleterious effects on anode performance.[66–69] According to thermodynamic



https://doi.org/10.1557/mrs.2014.170 Published online by Cambridge University Press

calculations by Sasaki,[76] $H_2S$ is the most stable sulphur-bearing species under SOFC operating conditions. Therefore, many researchers have investigated the effects of this species on anode performance. It is reported that exposing the Ni/YSZ cermet anode to $H_2S$ leads to decreased performance[66–68] and changes in the microstructure of Ni.[77] Sasaki et al.[48] calculated the phase diagram of C-H-O-Ni-S and showed that even with decreasing operating temperatures from 800°C to 600°C, $Ni_3S_2$ remains the most thermodynamically stable phase. It is worth bearing in mind, considering these calculated results, that different thermodynamics at the surface often make surfaces more reactive than the bulk material, and so sulfur poisoning could still occur at even lower SOFC operation temperatures.

Carbon deposition is another concern for long-term operation of SOFCs. Depending on the choice of fuel, residual carbon from fuel oxidation may deposit on the anode. Sasaki and Teraoka[70,71] calculated the C-H-O phase equilibrium diagram in the range of 100–1000°C, and found that the ratios between $H_2$, C, and oxygen atoms in the anode gas are key to preventing carbon deposition. According to that study, decreasing the temperature is thermodynamically disadvantageous in terms of preventing carbon deposition. However, there have been some reports of stable SOFC operation at low temperatures with negligible carbon deposition.[73] This suggests that the kinetics of carbon deposition (as opposed to the equilibrium thermodynamic approach of the calculations in References 70 and 71) can also play a role in preventing carbon deposition. Therefore, a well-balanced gas composition in terms of its proportions of C, H, and O atoms, and an anode material with sufficient catalytic activity to remove the deposited carbon is necessary to avoid carbon deposition under low-temperature SOFC operation.

One common approach to mitigate carbon deposition is by the use of certain additives to the anode. For example, Kim et al.[74] reported that the addition of Cu to Ni could prevent carbon deposition while giving reasonable electrochemical performance. Similarly, it has been reported that the addition of Sn to Ni/YSZ could also improve cell lifetime.[59,75] However, these electrochemical studies present a more "macroscopic" view of the device performance. The mechanisms by which these reduce the tendency for carbon decomposition, which is likely to be as a result of changes to the surface composition of the anode, have not yet been studied in much detail.

Overall, impurity segregation and (external) poisoning effects offer a rich area for the study of surface composition of SOFC anode materials and how they relate to electrochemical performance. In-depth characterization of these surface properties will allow the design of anode materials with improved tolerance to poisoning and carbon deposition at the lower temperatures of SOFC operation.

## Summary

SOFCs rely on mass and charge transport reactions across various surfaces and interfaces (e.g., oxidant/cathode, cathode/electrolyte, electrolyte/anode, and anode/fuel). We have discussed relevant aspects concerning the chemical composition of these interfaces, showing that surfaces cannot be regarded as a simple termination of the bulk structure. Often the electrochemically active surfaces are modified due to segregation of impurities or constituent cations, which affects the mass transport properties of the materials, electrochemical performance, and durability for low-temperature SOFC operation. With further understanding of these phenomena, the device lifetime and efficiency will be improved.

## Acknowledgments

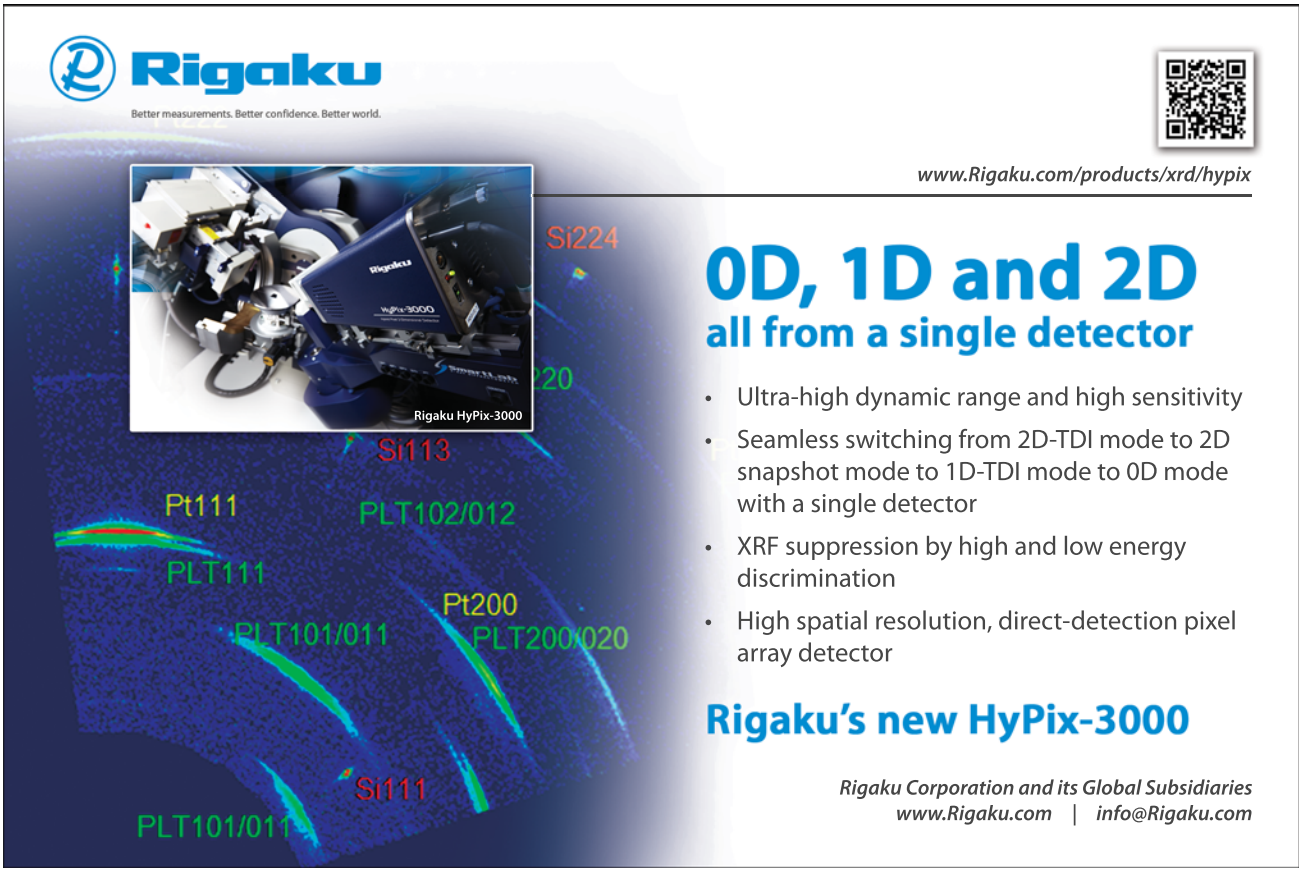
The authors gratefully acknowledge the support of the International Institute for Carbon Neutral Energy Research (wpi-I$^2$CNER), sponsored by the World Premier International Research Center Initiative (WPI), MEXT, Japan. Additionally, H.T. would like to thank the Japanese Society for the Promotion of Science for her post-doctoral fellowship.

## References

1. S.N. Shkerin, V. Kuznetsov, N.A. Kalashnikova, *Russ. J. Electrochem.* **39**, 591 (2003).
2. M. Aoki, Y.-M. Chiang, I. Kosacki, L.J.-R. Lee, H.L. Tuller, Y. Liu, *J. Am. Ceram. Soc.* **79**, 1169 (1996).
3. A.E. Hughes, S.P.S. Badwal, *Solid State Ionics* **46**, 265 (1991).
4. M. de Ridder, A.G.J. Vervoort, R.G. van Welzenis, H.H. Brongersma, *Solid State Ionics* **156**, 255 (2003).
5. P.J. Scanlon, R.A.M. Bink, F.P.F. van Berkel, G.M. Christie, L.J. van Ijzendoorn, H.H. Brongersma, R.G. van Welzenis, *Solid State Ionics* **112**, 123 (1998).
6. K.V. Hansen, K. Norrman, M. Mogensen, *Surf. Interface Anal.* **38**, 911 (2006).
7. Y. Oishi, Y. Sakka, K. Ando, *J. Nucl. Mater.* **96**, 23 (1981).
8. S. Litzelman, R. Souza, B. Butz, H. Tuller, M. Martin, D. Gerthsen, *J. Electroceram.* **22**, 405 (2009).
9. J. Druce, N. Simrick, T. Ishihara, J. Kilner, *Nucl. Instrum. Methods Phys. Res. B* **332** (2014).
10. Y. Wu, K. Vels Hansen, K. Norrman, T. Jacobsen, M.B. Mogensen, *ECS Trans.* **57**, 1673 (2013).
11. D. Ivanova, V.K. Andrei, V.K. Vladislav, F.M.B. Marques, *Bol. Soc. Esp. Ceram. Vidrio* **47**, 201 (2008).
12. T. Zhang, *Solid State Ionics* **168**, 187 (2004).
13. J. Druce, J. Kilner, *J. Electrochem. Soc.* **161**, F99 (2014).
14. M. de Ridder, R. van Welzenis, H. Brongersma, U. Kreissig, *Solid State Ionics* **158**, 67 (2003).
15. M. Guo, J. Lu, Y. Wu, Y. Wang, M. Luo, *Langmuir* **27**, 3872 (2011).
16. M.F. Wilkes, P. Hayden, A.K. Bhattacharya, *Appl. Surf. Sci.* **206**, 12 (2003).
17. H.B. Lee, F.B. Prinz, W. Cai, *Acta Mater.* **58**, 2197 (2010).
18. A. Ismali, J.B. Giorgi, T.K. Woo, *J. Phys. Chem. C* **116**, 704 (2012).
19. M.M. Kuklja, E.A. Kotomin, R. Merkle, Y.A. Mastrikov, J. Maier, *Phys. Chem. Chem. Phys.* **15**, 5443 (2013).
20. Y. Teraoka, N. Yamazoe, T. Seiyama, *J. Surf. Sci. Soc. Japan* **9**, 153 (1988).
21. M.M. Viitanen, R.G.V. Welzenis, H.H. Brongersma, F.P.F. van Berkel, *Solid State Ionics* **150**, 223 (2002).
22. E. Bucher, W. Sitte, F. Klauser, E. Bertel, *Solid State Ionics* **191**, 61 (2011).
23. J. Druce, T. Ishihara, J. Kilner, *Solid State Ionics* **262**, 893 (2014).
24. G. Vovk, X. Chen, C.A. Mims, *J. Phys. Chem. B* **109**, 2445 (2004).
25. M. Kubicek, A. Limbeck, T. Froemling, H. Hutter, J. Fleig, *J. Electrochem. Soc.* **158**, B727 (2011).
26. I.C. Fullarton, J.-P. Jacobs, H.E. van Benthem, J.A. Kilner, H.H. Brongersma, P.J. Scanlon, B.C.H. Steele, *Ionics* **1**, 51 (1995).
27. H. Dulli, P.A. Dowben, S.H. Liou, E.W. Plummer, *Phys. Rev. B: Condens. Matter* **62**, R14629 (2000).
28. S. Ponce, M.A. Peña, J.L.G. Fierro, *Appl. Catal. B* **24**, 193 (2000).
29. R. Bertacco, J.P. Contour, A. Barthélemy, J. Olivier, *Surf. Sci.* **511**, 366 (2002).
30. C.N. Borca, B. Xu, T. Komesu, H.K. Jeong, M.T. Liu, S.H. Liou, P.A. Dowben, *Surf. Sci.* **512**, L346 (2002).
31. J.A. Kilner, H. Tellez-Lozano, M. Burriel, S. Cook, J. Druce, *ECS Trans.* **57**, 1701 (2013).
32. H. Téllez, J. Druce, Y.-W. Ju, J. Kilner, T. Ishihara, *Int. J. Hydrogen Energy* (2014), doi: 10.1016/j.ijhydene.2014.06.102.


https://doi.org/10.1557/mrs.2014.170 Published online by Cambridge University Press

33. M. Sase, F. Hermes, K. Yashiro, K. Sato, J. Mizusaki, T. Kawada, N. Sakai, H. Yokokawa, *J. Electrochem. Soc.* **155**, B793 (2008).
34. M. Sase, K. Yashiro, K. Sato, J. Mizusaki, T. Kawada, N. Sakai, K. Yamaji, T. Horita, H. Yokokawa, *Solid State Ionics* **178**, 1843 (2008).
35. M.J. Gadre, Y.-L. Lee, D. Morgan, *Phys. Chem. Chem. Phys.* **14**, 2606 (2012).
36. Z. Feng, Y. Yacoby, M.J. Gadre, Y.-L. Lee, W.T. Hong, H. Zhou, M.D. Biegalski, H.M. Christen, S.B. Adler, D. Morgan, Y. Shao-Horn, *J. Phys. Chem. Lett.* **5**, 1027 (2014).
37. E.J. Crumlin, S.J. Ahn, D. Lee, E. Mutoro, M.D. Biegalski, H.M. Christen, Y. Shao-Horn, *J. Electrochem. Soc.* **159**, F219 (2012).
38. H. Ding, A.V. Virkar, M. Liu, F. Liu, *Phys. Chem. Chem. Phys.* **15**, 489 (2013).
39. W. Lee, J.W. Han, Y. Chen, Z. Cai, B. Yildiz, *J. Am. Chem. Soc.* **135**, 7909 (2013).
40. P.W. Tasker, *J. Phys. C: Solid State Phys.* **12**, 4977 (1979).
41. W.A. Harrison, *Phys. Rev. B: Condens. Matter* **83**, 155437 (2011).
42. E.J. Crumlin, E. Mutoro, Z. Liu, M.E. Grass, M.D. Biegalski, Y.-L. Lee, D. Morgan, H.M. Christen, H. Bluhm, Y. Shao-Horn, *Energy Environ. Sci.* **5**, 6081 (2012).
43. K. Min, C.W. Sun, W. Qu, X.G. Zhang, S. Yick, M. Robertson, C. Deces-Petit, R. Hui, *Int. J. Green Energy* **6**, 627 (2009).
44. S.-N. Lee, A. Atkinson, J.A. Kilner, *J. Electrochem. Soc.* **160**, F629 (2013).
45. X.B. Chen, Y.D. Zhen, J. Li, S.P. Jiang, *Int. J. Hydrogen Energy* **35**, 2477 (2010).
46. E. Bucher, M. Yang, W. Sitte, *J. Electrochem. Soc.* **159**, B592 (2012).
47. S.P. Jiang, X.B. Chen, *Int. J. Hydrogen Energy* **39**, 505 (2014).
48. K. Sasaki, K. Haga, T. Yoshizumi, D. Minematsu, E. Yuki, R. Liu, C. Uryu, T. Oshima, T. Ogura, Y. Shiratori, K. Ito, M. Koyama, K. Yokomoto, *J. Power Sources* **196**, 9130 (2011).
49. R.R. Liu, S.H. Kim, Y. Shiratori, T. Oshima, K. Ito, K. Sasaki, *ECS Trans.* **25**, 2859 (2009).
50. Y. Xiong, K. Yamaji, T. Horita, H. Yokokawa, J. Akikusa, H. Eto, T. Inagaki, *J. Electrochem. Soc.* **156**, B588 (2009).
51. A. Yan, M. Cheng, Y.L. Dong, W.S. Yang, V. Maragou, S.Q. Song, P. Tsiakaras, *Appl. Catal. B* **66**, 64 (2006).
52. K.F. Chen, J. Hyodo, L. Zhao, N. Ai, T. Ishihara, S.P. Jiang, *J. Electrochem. Soc.* **160**, F1033 (2013).
53. E. Bucher, C. Gspan, F. Hofer, W. Sitte, *Solid State Ionics* **238**, 15 (2013).
54. E. Bucher, C. Gspan, F. Hofer, W. Sitte, *Solid State Ionics* **230**, 7 (2013).
55. S.-N. Lee, A. Atkinson, J.A. Kilner, *ECS Trans.* **57**, 605 (2013).
56. A. Atkinson, S.A. Barnett, R.J. Gorte, J.T.S. Irvine, A. McEvoy, M.B. Mogensen, S.C. Singhal, J. Vohs, *Nat. Mater.* **3**, 17 (2004).
57. S. Jiang, S. Chan, *J. Mater. Sci.* **39**, 4405 (2004).
58. Y.-W. Ju, H. Eto, T. Inagaki, S. Ida, T. Ishihara, *J. Power Sources* **195**, 6294 (2010).
59. E. Nikolla, J. Schwank, S. Linic, *J. Electrochem. Soc.* **156**, B1312 (2009).
60. K. Norrman, K. Vels Hansen, M.B. Mogensen, *J. Eur. Ceram. Soc.* **26**, 967 (2006).
61. K. Vels Jensen, R. Wallenberg, I. Chorkendorff, M.B. Mogensen, *Solid State Ionics* **160**, 27 (2003).
62. A. Hauch, S.H. Jensen, J.B.B. Bilde-Sorensen, M.B. Mogensen, *J. Electrochem. Soc.* **154**, A619 (2007).
63. K. Vels Hansen, K. Norrman, M.B. Mogensen, *J. Electrochem. Soc.* **151**, A1436 (2004).
64. Y. Liu, C. Jiao, *Solid State Ionics* **176**, 435 (2005).
65. K. Haga, S. Adachi, Y. Shiratori, K. Itoh, K. Sasaki, *Solid State Ionics* **179**, 1427 (2008).
66. Y. Matsuzaki, I. Yasuda, *Solid State Ionics* **132**, 261 (2000).
67. Z. Cheng, S. Zha, M. Liu, *J. Power Sources* **172**, 688 (2007).
68. A. Hagen, J.F.B. Rasmussen, K. Thyden, *J. Power Sources* **196**, 7271 (2011).
69. A. Lussier, S. Sofie, J. Dvorak, Y.U. Idzerda, *Int. J. Hydrogen Energy* **33**, 3945 (2008).
70. K. Sasaki, Y. Teraoka, *J. Electrochem. Soc.* **150**, A878 (2003).
71. K. Sasaki, Y. Teraoka, *J. Electrochem. Soc.* **150**, A885 (2003).
72. S. McIntosh, R.J. Gorte, *Chem. Rev.* **104**, 4845 (2004).
73. Y.B. Lin, Z.L. Zhan, J. Liu, S.A. Barnett, *Solid State Ionics* **176**, 1827 (2005).
74. H. Kim, C. Lu, W.L. Worrell, J.M. Vohs, R.J. Gorte, *J. Electrochem. Soc.* **149**, A247 (2002).
75. H. Kan, H. Lee, *Appl. Catal. B* **97**, 108 (2010).
76. K. Sasaki, *J. Fuel Cell Sci. Technol.* **5** (3), 031212 (2008).
77. J. Dong, Z. Cheng, S.W. Zha, M.L. Liu, *J. Power Sources* **156**, 461 (2006). □






https://doi.org/10.1557/mrs.2014.170 Published online by Cambridge University Press

# 2015 MRS® SPRING MEETING & EXHIBIT

**April 6–10, 2015 | San Francisco, California**

# CALL FOR PAPERS

**Abstract Submission Opens September 23, 2014 | Abstract Submission Deadline October 23, 2014**

## Energy

- A Emerging Silicon Science and Technology
- B Thin-Film Compound Semiconductor Photovoltaics
- C Perovskite Solar Cells
- D Organic-Based Photovoltaics
- E Advanced Solar Cells—Components to Systems
- F Biohybrid Solar Cells—Photosynthesis-Based Photovoltaics and Photocatalytic Solar Cells
- G Next-Generation Electrochemical Energy Storage and Conversion Systems—Synthesis, Processing, Characterization and Manufacturing
- H Mechanics of Energy Storage and Conversion—Batteries, Thermoelectrics and Fuel Cells
- I High Capacity Anode Materials for Lithium Ion Batteries
- J Latest Advances in Solar Water Splitting
- K The Development of Oxygen Reduction Reaction (ORR) and Oxygen Evolution Reaction (OER) Materials in Energy Storage and Conversion Systems

## Nanomaterials

- L Bioinspired Micro- and Nano-Machines—Challenges and Perspectives
- M Nanoscale Heat Transport—From Fundamentals to Devices
- N From Molecules to Colloidal Compound Semiconductor Nanocrystals—Advances in Mechanism-Enabled Design and Syntheses
- O Emerging Non-Graphene 2D Materials
- P Nanogenerators and Piezotronics
- Q Externally Actuated Responsive Nanomaterials—Design, Synthesis, Applications and Challenges
- R Photoactive Nanoparticles and Nanostructures
- S Semiconductor Nanowires and Devices for Advanced Applications
- T Graphene and Carbon Nanotubes

## Electronics and Photonics

- U The Interplay of Structure and Carrier Dynamics in Energy-Relevant Nanomaterials
- V Resonant Optics—Fundamentals and Applications
- W Light-Matter Processes in Molecular Systems and Devices
- Y Phase-Change Materials for Data Storage, Cognitive Processing and Photonics Applications
- Z Plasmonics and Metamaterials—Synthesis, Characterization and Integration
- AA Materials for Beyond the Roadmap Devices in Logic, Power and Memory
- BB Innovative Interconnects/Electrodes for Advanced Devices, Flexible and Green-Energy Electronics
- CC Reliability and Materials Issues of Semiconductors—Optical and Electron Devices and Materials III
- DD Tailored Disorder—Novel Materials for Advanced Optics and Photonics
- EE Quantum Photonics, Information Technology and Sensing
- FF Defects in Semiconductors—Relationship to Optoelectronic Properties

## Soft and Biomaterials

- GG Foundations of Bio/Nano Interfaces—Synthesis, Modeling, Design Principles and Applications
- HH Supramolecular Materials—Assembly and Dynamics
- II Organic Bioelectronics—Materials, Processes and Applications
- JJ Exploiting Bioinspired Self-Assembly for the Design of Functional and Responsive Materials
- KK Nanomaterials in Translational Medicine
- LL Soft Electronics—From Electronic Skin to Reliable Neural Interfaces
- MM Crystal Engineering—Design, New Materials and Applications

## General—Fabrication and Characterization

- NN Adaptive Architecture and Programmable Matter—Next-Generation Building Skins and Systems from Nano to Macro
- OO Metal-Assisted Chemical Etching of Silicon and Other Semiconductors
- PP Gold-Based Materials and Applications
- QQ Plasma-Based Materials Science and Engineering
- RR Solution Syntheses of Inorganic Functional/Multifunctional Materials
- SS Oxide Thin Films and Nanostructures for Advanced Electrical, Optical and Magnetic Applications
- TT Metal Oxides—From Advanced Fabrication and Interfaces to Energy and Sensing Applications
- UU Titanium Oxides—From Fundamental Understanding to Applications
- VV Science and Technology of Superconducting Materials
- WW Ultrafast Dynamics in Complex Functional Materials
- XX Multiscale Modeling and Experiments on Microstructural Evolution in Nuclear Materials
- YY Insights for Energy Materials Using *In-Situ* Characterization
- ZZ Materials Information Using Novel Techniques in Electron Microscopy

**www.mrs.org/spring2015**

### Meeting Chairs

**Artur Braun** Swiss Federal Laboratories for Materials Science and Technology
**Hongyou Fan** Sandia National Laboratories
**Ken Haenen** Hasselt University and IMEC vzw
**Lia Stanciu** Purdue University
**Jeremy A. Theil** Quantumscape, Inc.

### Don't Miss These Future MRS Meetings!

**2015 MRS Fall Meeting & Exhibit**
November 29 – December 4, 2015
Hynes Convention Center & Sheraton Boston Hotel
Boston, Massachusetts

**2016 MRS Spring Meeting & Exhibit**
March 28 – April 1, 2016
Phoenix Convention Center
Phoenix, Arizona

MRS MATERIALS RESEARCH SOCIETY®
*Advancing materials. Improving the quality of life.*
506 Keystone Drive • Warrendale, PA 15086-7573
Tel 724.779.3003 • Fax 724.779.8313
info@mrs.org • www.mrs.org

https://doi.org/10.1557/mrs.2014.170 Published online by Cambridge University Press